Parametric decay instabilities of microwave beams in fusion plasmas: occurrence, consequences and new possibilities

Plasma Physics and Controlled Fusion

OPEN ACCESS

RECEIVED
10 November 2025

REVISED
29 January 2026

ACCEPTED FOR PUBLICATION
17 April 2026

PUBLISHED
11 May 2026

PAPER

Parametric decay instabilities of microwave beams in fusion plasmas: occurrence, consequences and new possibilities

S K Nielsen[1,*], A Clod[1], M Senstius[2], R Ragona[1], J K de Wit[1], S K Hansen[3], J Rasmussen[1], J Stober[4], S Coda[5], D Moseev[6], the ASDEX Upgrade Team[4,7], the TCV Team[5,8], the W7-X Team[4,9], the NORTH Team[1,10] and the EUROfusion WPTE Team[11]

[1] Department of Physics, Technical University of Denmark, DK-2800 Kgs. Lyngby, Denmark
[2] Rudolf Peierls Centre for Theoretical Physics, University of Oxford, Oxford OX1 3NP, United Kingdom
[3] Plasma Science and Fusion Center, Massachusetts Institute of Technology, Cambridge, MA 02139,United States of America
[4] Max-Planck-Institut für Plasmaphysik, Garching b. München, Germany
[5] École Polytechnique Fédérale de Lausanne (EPFL), Swiss Plasma Center (SPC), CH-1015 Lausanne, Switzerland
[6] Max-Planck-Institut für Plasmaphysik, Greifswald, Germany
[7] See Zohm *et al* 2024 (https://doi.org/10.1088/1741-4326/ad249d) for the ASDEX Upgrade Team.
[8] See Reimerdes *et al* 2022 (https://doi.org/10.1088/1741-4326/ac369b) for the TCV Team.
[9] See Grulke *et al* 2024 (https://doi.org/10.1088/1741-4326/ad2f4d) for the W7-X Team.
[10] See Nielsen *et al* 2021 (https://doi.org/10.1016/j.fusengdes.2021.112288) for the NORTH Team.
[11] See Joffrin *et al* 2024 (https://doi.org/10.1088/1741-4326/ad2be4) for the EUROfusion WPTE Team.
[*] Author to whom any correspondence should be addressed.

E-mail: skni@fysik.dtu.dk

Keywords: electron cyclotron resonance heating, parametric decay instabilities, plasma, tokamak, collective Thomson scattering, two plasmon decay

Abstract

Electron cyclotron heating by high-power microwave beams is a key method for plasma heating in tokamaks and stellarators. Under some conditions, these beams engage in nonlinear three-wave interactions, known as parametric decay instabilities (PDIs), where energy is transferred from the main beam to two downshifted waves. PDIs are well documented to occur during fundamental electron Bernstein wave heating, with observations in multiple devices. However, PDIs were overlooked in the more common second-harmonic electron cyclotron heating until recently, when nonlinear scattering was observed. This has been attributed to a class of absolute PDIs that involves wave trapping in density fluctuations. Here we provide an overview of recent numerical and experimental results in the study of PDIs. We show direct observations of PDIs at the devices ASDEX Upgrade, TCV, Wendelstein 7-X, and NORTH, and show that the occurrence of PDIs is correlated with density fluctuations in the scrape-off layer caused by edge localized modes and blobs as well as density fluctuations in the plasma core due to NTMs. We outline the consequences of PDI occurrence, which could include a decrease in heating efficiency and an associated fast-ion production. In addition, we discuss possible schemes for exploiting PDIs, including controlled energy transfer to selected plasma waves and potential diagnostic techniques for density fluctuations.

1. Introduction

Electron cyclotron resonance heating (ECRH) has long been a cornerstone of plasma heating and current drive in magnetic confinement fusion devices [1]. Its precision and localization make it particularly valuable for controlling magnetohydrodynamic (MHD) instabilities and tailoring plasma profiles. However, over the past two decades, a growing body of experimental and theoretical work has revealed that ECRH in some cases is susceptible to nonlinear wave–plasma interactions, most notably parametric decay instabilities (PDIs), which can potentially alter the expected behavior of the injected microwave power.

PDIs occur when a high-power electromagnetic pump wave decays into two or more daughter waves, typically under conditions of reduced group velocity or wave trapping. In the context of second-harmonic ECRH, this often involves the decay of an X-mode wave into two upper hybrid (UH) waves near half the ECRH frequency. These UH waves can become trapped in regions of non-monotonic electron density—such as near the O-point of rotating or locked MHD modes—leading to strong secondary instabilities and anomalous microwave emissions [2].

Experimental observations from devices such as ASDEX Upgrade, TEXTOR, and TCV have demonstrated that these PDIs can cause significant diagnostic interference and even physical damage to microwave systems. In some cases, up to 80% of the injected ECRH power has been predicted to be diverted into daughter waves, which could in principle alter the heating profile and reduce the efficiency of current drive [3]. Theoretical models [4, 5] and PIC simulations [6, 7] have further refined our understanding of the threshold conditions for PDI onset, emphasizing the role of magnetic islands, density gradients, and harmonic resonance layers.

This article reviews the key developments in the study of parametric decay of ECRH waves in tokamak and stellarator plasmas over the past twenty years. We synthesize the main findings from experimental campaigns and numerical simulations to provide a comprehensive overview of the mechanisms, diagnostics, and implications of PDIs in fusion-relevant conditions.

2. Background

In a linear medium, an electromagnetic wave induces a current that is proportional to the field amplitude. This leads to a linear wave equation, implying that different waves propagate independently of one another. In contrast, in a nonlinear medium, the induced current depends nonlinearly on the electric field amplitude, resulting in a nonlinear wave equation. Under such conditions, waves with different frequencies and wave numbers can interact, allowing energy transfer between them.

Waves used for ECRH are launched outside the plasma and propagate to a cyclotron resonance layer typically close to the plasma center. When describing the propagation of these heating waves away from resonances, the non-linear contribution of the induced current can often be neglected, and wave propagation within a linear medium can be assumed. However, this assumption can break down under certain conditions to be discussed here.

The PDI is a three-wave interaction that results from a quadratic nonlinearity where energy is transferred from a primary wave, often called a pump wave, into two secondary waves, often called daughter waves. For this process to be efficient, the angular frequency, ω, and the wavenumber, $\mathbf{k}$, must be approximately conserved. This can be written as the phase-matching conditions

$$\mathbf{k}_0 \approx \mathbf{k}_1 + \mathbf{k}_2, \qquad \omega_0 \approx \omega_1 + \omega_2. \tag{1}$$

Here, subscript 0 refers to the pump wave, and 1,2 to the daughter waves.

A general condition for the occurrence of PDIs, i.e. for the interactions to become unstable, is that the interacting waves must exceed a certain power threshold. Due to spatial gradients in plasma parameters, the wave numbers of the involved waves often vary, meaning that the PDI matching condition is typically satisfied only within a narrow spatial region. This is illustrated in figure 1(a), where the pump wave transfers energy to the daughter waves only within a finite region. The resulting energy transfer is limited and is referred to as convective PDI. Typically, convection through the interaction region is a stronger suppression mechanism of the instability than linear wave damping.

On the other hand, if the daughter waves can return to the interaction region multiple times, as illustrated in figure 1(b), more energy can be transferred to them. When daughter waves are trapped and the PDI matching condition is satisfied within the trapping region, the daughter waves can grow exponentially over time. This phenomenon is known as an absolute PDI and can lead to a significant reduction in the instability power threshold [8].

The two methods that are most commonly used to model PDIs in plasmas are kinetic particle-in-cell (PIC) simulations and coupled mode equations based on WKB theory. The latter approach will not be covered here, but is discussed in, e.g. [5, 9, 10].

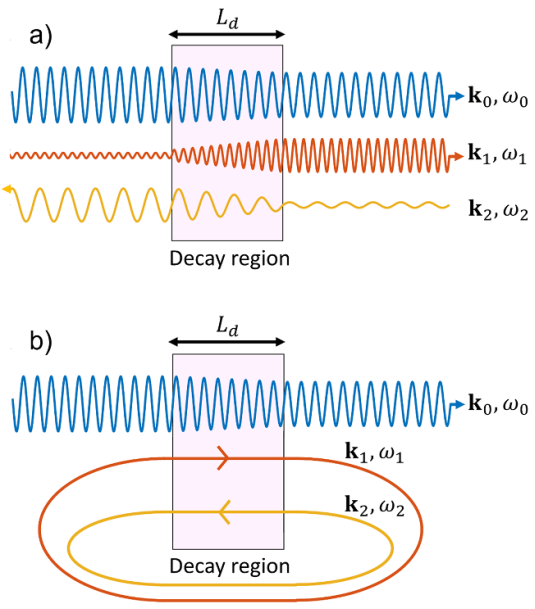

Figure 1. Illustration of the two types of parametric decay instabilities. Blue color indicates the pump wave, red and yellow the daughter waves. (a) Convective instability with a finite energy transfer to daughter waves. (b) Absolute instability with exponential growth of daughter waves in time.

3. PIC simulations of PDIs

3.1. Convective PDIs near the UH layer

Under most conditions, the power levels used for ECRH in tokamaks and stellarators are orders of magnitude below the PDI power threshold. However, when an X-mode wave approaches the UH layer, i.e. where the wave frequency equals the UH frequency $f_{\mathrm{uh}} = \sqrt{\omega_{\mathrm{pe}}^2 + \omega_{\mathrm{ce}}^2}/2\pi$, the wave is slowed down and linearly converted to a backward propagating electron Bernstein wave (EBW), which has a much lower group velocity than the X-mode wave. Here, we use the usual definitions of the plasma frequency squared as $\omega_{\mathrm{pe}}^2 = n_{\mathrm{e}} q_{\mathrm{e}}^2/(m_{\mathrm{e}}\epsilon_0)$ and the cyclotron frequency as $\omega_{\mathrm{ce}} = q_{\mathrm{e}}B/m_{\mathrm{e}}$. Both the X-mode wave approaching the UH layer and the linearly converted EBW can engage in PDIs. To demonstrate this, a PIC simulation of an X-EBW conversion is carried out in a 1D domain. The incoming X-mode wave has a frequency of 105 GHz and a very modest intensity of 11.6 kW cm^{-2}. Additional details of the simulation can be found in [10]. The assumed background density profile and evolution of the longitudinal wave electric field, E_x, in space and time are shown in figure 2. The background magnetic field is constant pointing in the z-direction, and the X-mode wave gradually approaches the UH resonance at $x =$ 26 mm. To investigate PDIs in the simulation, a 2D fast Fourier transformation (FFT) of E_x has been computed within three different spatio-temporal windows. In the first 2D FFT, shown in figure 3, the pump X-mode wave has not yet converted to an EBW. The second 2D FFT taken at the UH layer at a later time is plotted in figure 4 and shows how a convective PDI occurs when the X-mode wave is located at the turning point, where its local group velocity goes to zero. Although a resonant decay satisfying the phase-matching conditions (equation (1)) is not possible, the field amplification of the pump wave is strong enough to initiate a PDI into an EBW propagating towards higher x (forward propagating) and a non-propagating quasi-mode. The longitudinal electric field of the forward propagating EBWs can be seen to the right of the UH resonance in figure 2(b).

The fraction of the pump wave not lost due to this PDI converts linearly to an EBW that propagates away from the UH layer. When a 2D FFT is taken further away from the UH layer as shown in figure 5, this EBW is seen to be involved in a different class of convective PDIs. These PDIs consist of multiple coupled Stokes and anti-Stokes processes, generating both upshifted EBWs, downshifted EBWs, and a high-harmonic ion Bernstein wave on the lower hybrid wave branch. A detailed analysis of this class of PDIs is found in [10].

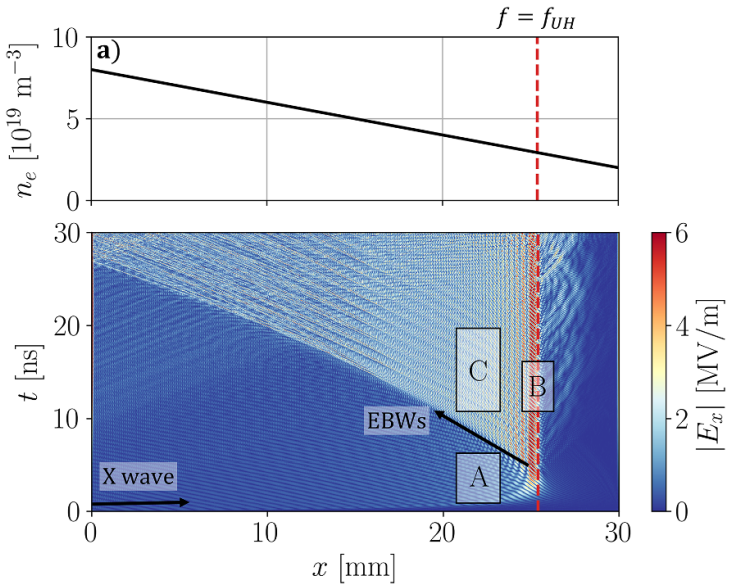

Figure 2. Results of PIC simulations of X-EBW conversion (a) assumed 1D background density profile. (b) Longitudinal electric field in (x), (t) space. The red dashed line marks the UH layer and the two arrows indicate the injected slow X wave and the EBWs generated at the UH layer. The regions A, B, and C represent the 2D FFT windows used in the figures 3–5, respectively.

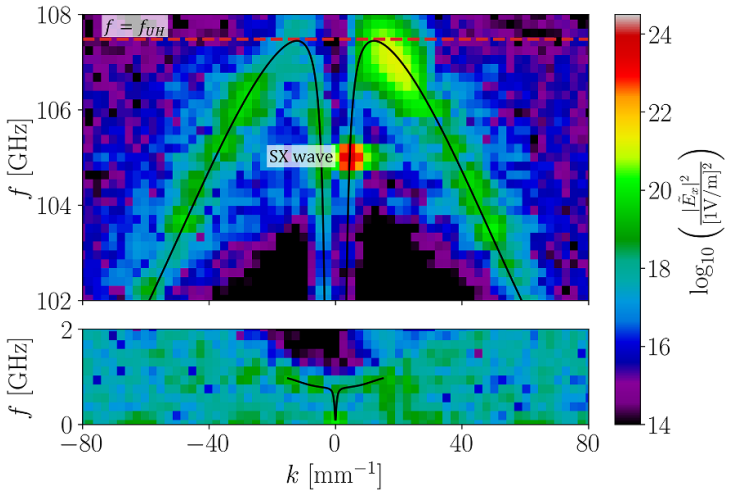

Figure 3. 2D FFT of the longitudinal wave electric field, E_x within the window A in figure 2. The solid black lines show the dispersion curves for the slow X-mode (SX), EBW, and lower hybrid wave.

3.2. Absolute PDIs near the second-harmonic UH layer

Waves near the UH frequency can be partially trapped in non-monotonic density profiles. This happens because UH waves can be localized between several UH layers, which they are unable to pass, in such a profile. The UH waves can therefore form quantized modes which are superpositions of forward propagating X-mode waves and backward propagating EBWs that couple to each other near the UH layers. This mechanism works even at low mode numbers, enabling trapping in density structures down to the mm range in typical tokamak plasmas [11].

If an injected ECRH wave propagates through such a non-monotonic density structure near the second-harmonic UH layer, it can couple to a pair of trapped UH waves. This is primarily of concern for second-harmonic X-mode heating and current drive. Since the convection of the daughter waves of the interaction region is low, the instability can grow exponentially in time. This absolute instability can be suppressed by collisions and diffraction of the daughter waves out of the interaction region. However, with only these effects, the power threshold is typically substantially reduced.

The exponential growth of the trapped daughter waves eventually saturates due to secondary instabilities. Typically the amplitudes of the primary daughter waves exceed a threshold for a PDI involving a downshifted UH wave and an ion wave, as was discussed in section 3.1. A dynamic cascade of such

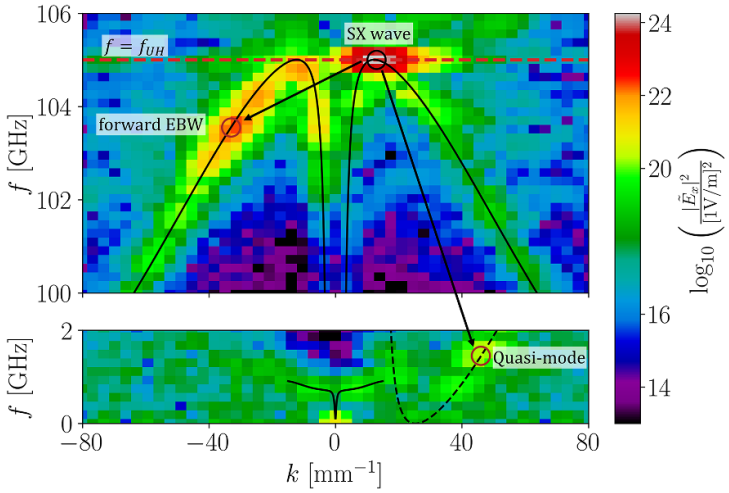

Figure 4. 2D FFT of the longitudinal electric field in window B in figure 2. The solid black lines show the dispersion curves for the X-mode, EBW, and lower hybrid wave, and the solid dashed line shows all quasi-modes satisfying the selection rules for PDIs where the SX-mode couples to a downshifted forward propagating EBW. Several of this type of convective PDIs appear to be occurring with the circles and arrows marking the most prominent one.

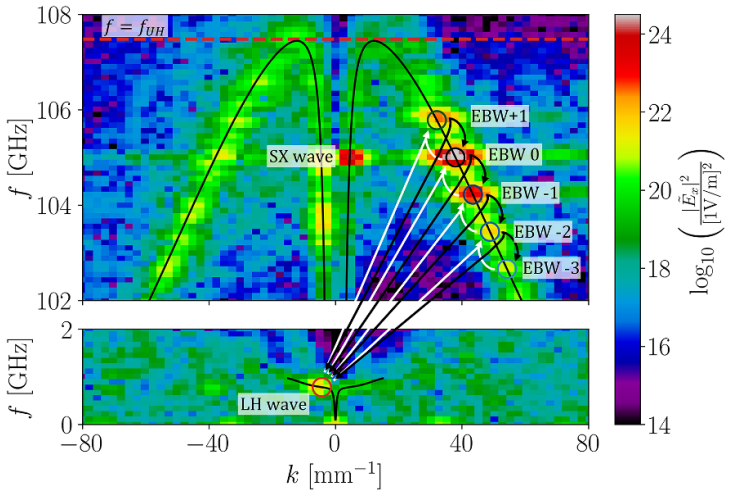

Figure 5. 2D FFT of the longitudinal electric field in window C in figure 2. The solid black lines show the dispersion curves for the X-mode, EBW, and lower hybrid wave. The colored circles mark the linearly converted EBW (denoted EBW 0) as well as a range of upshifted and downshifted EBWs satisfying the selection rules for PDIs involving a lower hybrid wave, marked with a red circle. The black arrows indicate Stokes processes, and the white arrows indicate anti-Stokes processes.

decays can follow until the downshifted UH daughter waves are able to escape the non-monotonic structure. The waves of the cascade can also recombine into waves with frequencies close to that of the ECRH pump wave. Figure 6(a) shows an illustration of waves and interactions in such a cascade, and figure 6(b) shows how a cascade can terminate after a few subsequent decays.

This model was first suggested in [8] and has often been referred to as an absolute two-plasmon decay (TPD) instability. The model has since been discussed and expanded upon in various primarily analytical papers [3–5], as well as a number of numerical papers where the quantization of UH modes and growth rates of the reduced models are tested against PIC simulations [7, 11–13].

A demonstration of the TPD cascade is shown in figure 7, where a 1D simulation was carried out to assess the TPD under plasma conditions relevant to the NORTH tokamak. The simulation was performed with the fully kinetic PIC code EPOCH [14]. The plasma consisted of electrons and a single ion species, modeled as hydrogen. Both species were initialized with a non-monotonic density profile and a uniform temperature of 5 eV. The system used 3300 grid cells with 12 000 superparticles per cell and was immersed in a perpendicular magnetic field of 0.09 T. A transversely polarized 5.8 GHz wave with a large intensity of 1 kW cm^{-2} was continuously injected from the left boundary. This configuration led to wave

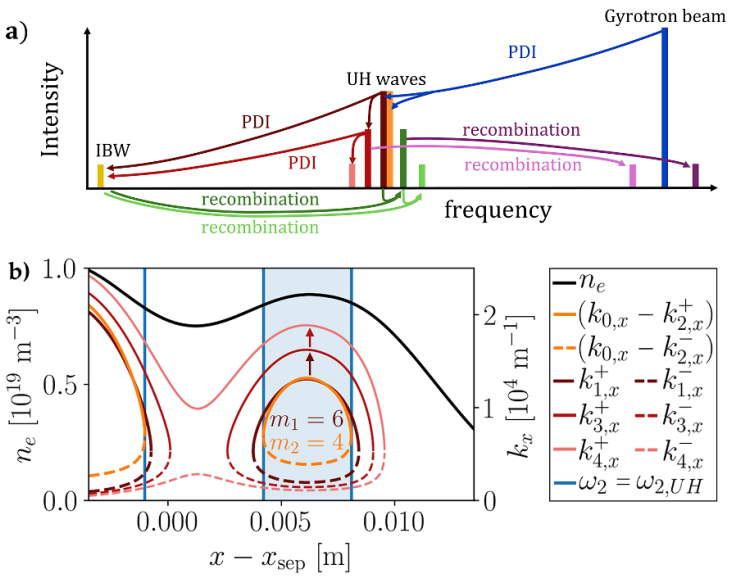

Figure 6. (a) Schematic of the two plasmon decay instability chain. In the primary absolute PDI, the pump wave decays into two trapped UH waves with amplitudes growing exponentially in time. When the amplitude of the primary UH waves becomes sufficiently large, the primary decay saturates due to a series of parametric instabilities of the type shown in figure 5, where energy gets divided among downshifted and upshifted UH waves and a high-harmonic ion Bernstein wave. This decay chain can continue until some UH waves are no longer trapped, which introduces convective losses. Additional recombination processes generate radiation around the gyrotron frequency. (b) Schematic of a non-monotonic density profile (black) that can act as a trapping structure for daughter waves. Remaining contours show the wavenumbers of the daughter waves. The superscript + marks their electron Bernstein component and the − marks the X-mode. Once an UH wave (ω_4, k_4) is no longer trapped, the PDI chain will terminate, and the decay wave may travel towards the plasma center.

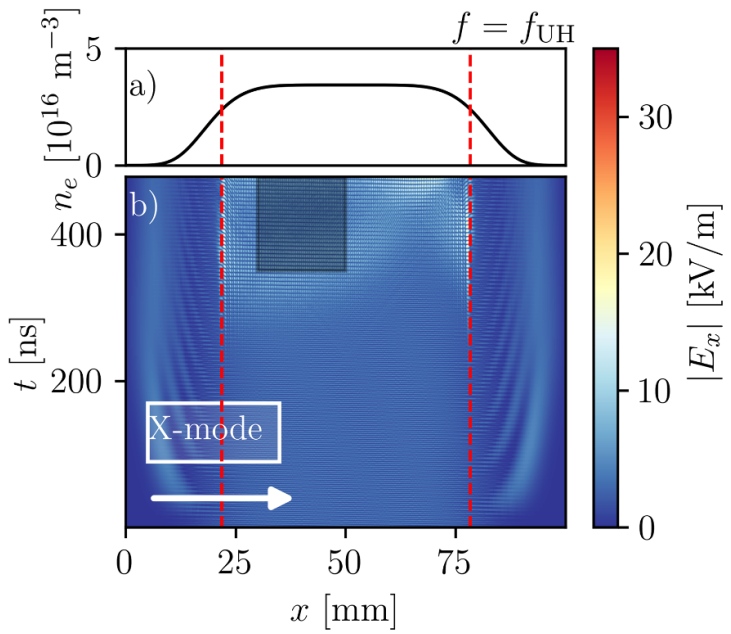

Figure 7. Overview of a 1D PIC simulation used to study TPD. Panel (a) shows the electron number density as a function of space. The ions, modeled as hydrogen, have the same densities. The red lines show the UH layer. (b) The longitudinal electric field component as a function of space and time. The shaded region marks the spatiotemporal window for the 2D FFT shown in figure 8.

trapping of EBWs near half the injected wave's frequency. The boundaries were set to absorb electromagnetic fields and to re-inject any escaping particles in a thermalized state. The longitudinal electric field component can be seen to increase within the UH layers of the profile after 300 ns, indicating parametric excitation of the daughter waves.

Figure 8 shows the 2D FFT of the longitudinal electric field into (f, k)-space from the simulation in figure 7. The transform uses a temporal window $t \in [350, 450]$ ns and a spatial window of $x \in$

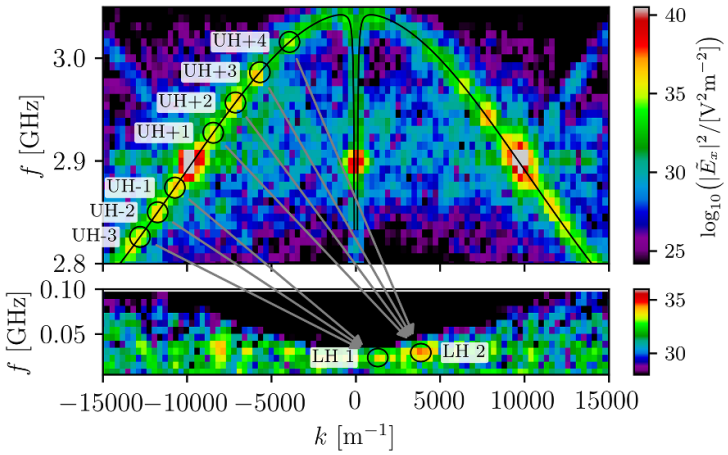

Figure 8. The 2D FFT into (f, k)-space of the longitudinal electric field component shown in figure 7. Panel (a) shows frequency- and wavenumber ranges around the trapped EBWs, and the circles highlight excited UH waves from both the Stokes and anti-Stokes processes. The black lines show the dispersion curves for the X-mode and EBW branch. Panel (b) shows the lower hybrid wave frequency range, and the circles highlight the two excited lower hybrid waves from the instability.

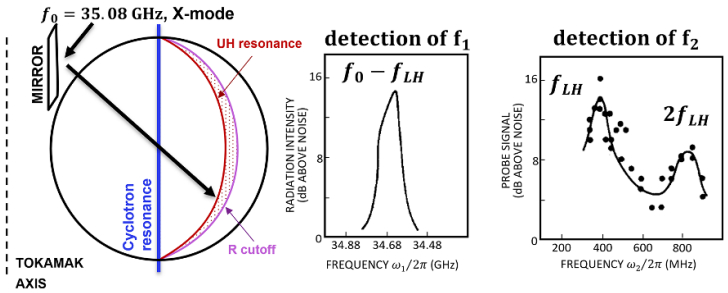

Figure 9. Left: geometry of the Versator II tokamak with X-mode injection from the high field side. Once the X-mode reached the UH resonance after passing the optically thin cyclotron resonance the beam was subject to convective PDI. Center: measured high frequency daughter wave. Right: measured low frequency daughter wave. Adapted from [15], with the permission of AIP Publishing.

[30, 50] mm. Two strong signals near 2.90 GHz are evident, and they correspond to the primary daughter waves excited by the instability. They appear on the Bernstein branch as well as in their X-mode component at small wavenumbers. The subsequent decays into frequency-downshifted EBWs and lower hybrid waves are visible, as well as anti-Stokes processes with another lower hybrid wave into upshifted waves.

4. Experimental evidence of PDIs

4.1. Convective PDIs near the UH layer

The experimental observation of convective PDIs near the UH layer was first reported from the Versator II tokamak [15] where an X-mode beam was injected from the high-field side as shown in figure 9. The X-mode is only weakly absorbed by the fundamental electron cyclotron resonance and is then linearly converted into EBWs at the UH resonance. A radiometer measured clear escaping waves downshifted by a lower hybrid frequency from the injected pump wave corresponding to the EBW daughter wave, and a loop antenna picked up signatures of the daughter waves in the vicinity of the lower hybrid frequency. Similar results have been reported at a number of devices, such as W7-AS and TJ-K, also during EBW O-X-B conversion where the final conversion point is similar to the scenario from Versator II [16–18].

A detailed study of the convective PDI was recently reported from ASDEX Upgrade where O-mode waves were injected from the low-field side and partly converted into X-mode upon reflection at the high-field side wall. By changing the plasma parameters the fractional X-mode power that reached the UH resonance was varied and the predicted power thresholds were experimentally validated [19]. In figure 10 the measured spectra are presented for varying power levels reaching the UH resonance. In

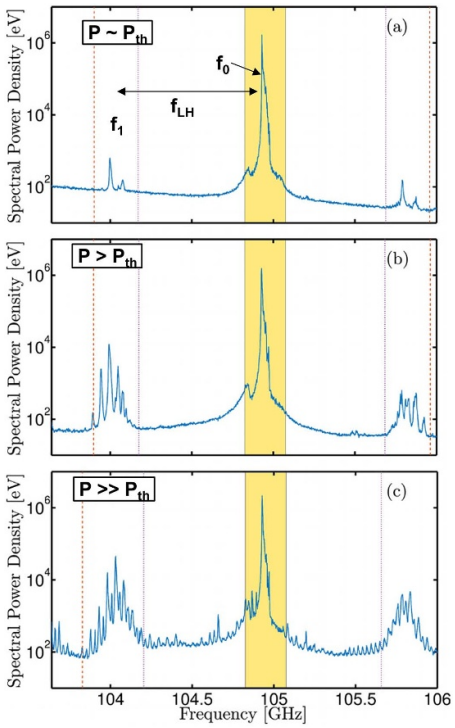

Figure 10. Escaping microwave signals near the pump frequency in ASDEX upgrade during convective PDI experiments. Reprinted from [19], with the permission of AIP Publishing.

figure 10(a) signatures of up- and down- shifted daughter waves appear when the power is just above the theoretical power threshold P_{th}. When the power is increased further (figure 10(b)) more harmonics of the ion Bernstein waves appear, and for yet further increases in power the process seems to saturate and a complex spectrum of daughter waves appears.

4.2. Absolute PDIs near the second-harmonic UH layer

The theory of TPD was first proposed in 2015 [8] to explain observations of anomalous scattering at the TEXTOR tokamak at frequencies near the gyrotron frequency [2, 20]. The TEXTOR results revealed strong signals emitted from the plasma near the ECRH gyrotron frequency, which were correlated with the passing of the O-point of a rotating magnetic island through the gyrotron beam. The clear identification of the magnetic island position close to the location of the UH resonance at half the gyrotron frequency led to the hypothesis that half-frequency waves were generated via TPD.

The location of the second-harmonic UH resonance layer, where a non-monotonic density perturbation would facilitate the TPD, depends on the magnetic field and density profile. To illustrate the location, figure 11 shows the location of the second-harmonic UH resonance for 140 GHz for an ASDEX Upgrade equilibrium at 2.5 T with varying central electron density. At zero density the second-harmonic UH resonance coincides with the second-harmonic electron cyclotron resonance but moves further towards the plasma edge for increasing density. Thus at low density, PDI may be generated in the plasma center and at high density at the plasma edge.

The experimental confirmation of the above hypothesis was achieved at ASDEX Upgrade, where a radiometer observed the microwaves escaping the plasma in the spatial vicinity of the gyrotron, near 70 GHz, during heating with 140 GHz X-mode ECRH [21]. An example from ASDEX Upgrade is shown in figure 12. Here, a radiometer channel centered at 69.6 GHz with a bandwidth of 80 MHz is shown, alongside a 139.7 GHz channel and a measurement of the ion saturation current in the divertor region. Sudden drops in the ion saturation current indicate edge localized mode (ELM) events, which show a strong correlation with both radiometer signals. A comprehensive analysis of all radiometer channels is presented in [21], which also includes MHD simulations of ELM events demonstrating that trapping of 70 GHz daughter waves in the associated density perturbations lowers the PDI threshold well below the injected power levels.

When the UH resonance is placed at mid radius, as illustrated in figure 11(b), density perturbations associated to magnetic islands may result in TPD and generate waves as illustrated in figure 6(a). The signals at half of the gyrotron frequency have so far been observed both on ASDEX Upgrade and TCV

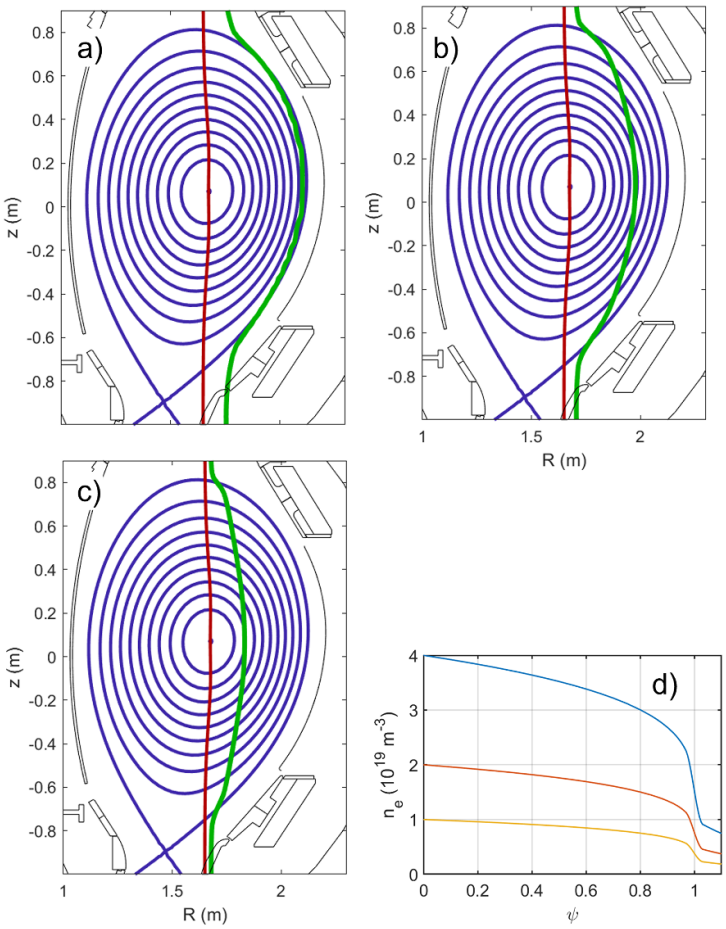

Figure 11. Location of the 140 GHz second-harmonic UH resonance for three different density profiles. (a) Core $n_e = 4 \times 10^{19}\,m^{-3}$, (b) $n_e = 2 \times 10^{19}\,m^{-3}$, and (c) $n_e = 1 \times 10^{19}\,m^{-3}$. The density profiles are shown in (d).

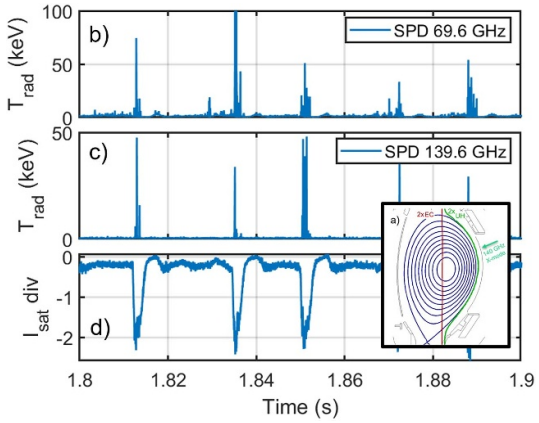

Figure 12. Experimental evidence for generation of daughter waves at half the frequency of the pump wave from ASDEX Upgrade, with the location of relevant resonances shown in (a). The intensity of half-frequency decay waves (b) and of signals just below the ECRH frequency (c) both correlate well with ion saturation currents in the divertor (d) that indicate the times of ELM events.

during rotating magnetic islands [22]. The recombination waves centered around the gyrotron frequency have frequently been observed at the TEXTOR [20] and ASDEX tokamaks [22], and examples of the frequency spectra are presented in figure 13.

Since rotating magnetic islands are highly dynamic, the associated TPDI signal is seen to vary in time as the island moves. We note that time evolution of the magnetic islands is typically much slower than the inverse growth rate of the TPDI. When the O-point of the magnetic island passes in front of the gyrotron launcher, the resulting density perturbation typically enables wave trapping. As the island

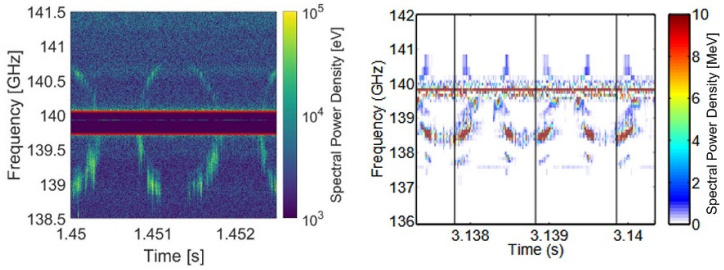

Figure 13. Example of measured recombination of PDI daughter waves when applying second-harmonic 140 GHz X-mode ECRH during rotating magnetic islands in ASDEX-Upgrade #35 186 (left) and TEXTOR #108 115 (right). The location of the second-harmonic UH resonance at 140 GHz is, in both cases, close to the island O-point. Reproduced from [22]. © IOP Publishing Ltd. All rights reserved. Reproduced from [20]. © The Author(s). Published by IOP Publishing Ltd. CC BY 4.0.

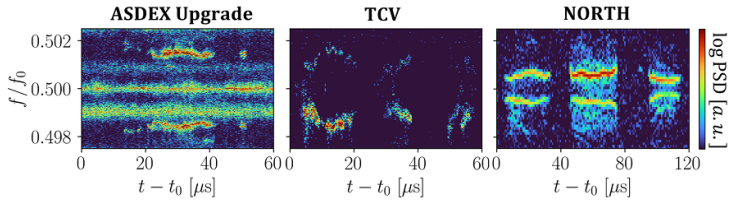

Figure 14. Time and frequency resolved measurements of TPD waves near half the ECRH frequency for ASDEX Upgrade [$R = 1.65$, $B = 2.6$ T] (left), TCV [$R = 0.8$ m, $B = 1.2$ T, and NORTH [$R = 0.25$ m, $B = 0.1$ T].

continues to rotate both toroidally and poloidally, the trapping conditions change, and eventually no trapping is possible when the island's X point aligns with the gyrotron launcher position. This dynamic evolution disrupts the TPDI process and leads to intervals without detectable TPDI signals, as shown in figure 13.

The TPD process has been confirmed in very different tokamak environments. Recently, results from the tokamak NORTH [23] also showed decay waves at half the heating frequency during second-harmonic heating. Operating with a toroidal magnetic field of 0.1 T, NORTH uses a 5.8 GHz magnetron for second-harmonic heating [24]. Due to the low plasma temperature in NORTH (5–15 eV), the parametrically induced waves can be measured directly using Langmuir probes inside the plasma. Figure 14 shows examples of measured TPD waves in ASDEX Upgrade, TCV, and NORTH. Since the frequency is normalized to the ECRH frequency, it is evident that the dynamics of the decay waves in all three devices exhibit similar behavior both with respect with frequency separation and timing. This is remarkable, considering that the plasma parameters differ significantly across the devices. In particular, the densities, temperatures, and magnetic fields vary by several orders of magnitude in the three devices. This observation further motivates TPD experiments in smaller devices, as they can provide valuable insights into the TPD processes occurring in larger systems such as ASDEX Upgrade and ITER at reduced cost and complexity.

Measurements have also been performed at the Wendelstein 7-X stellarator. Here, powerful signals with frequencies near the gyrotron frequency—close to 140 GHz—were observed to exhibit strong nonlinear behavior with respect to gyrotron power [25]. It was identified that the signals originated from PDI of the ECRH beam in the non-monotonic density profile at the divertor mangetic island in front of the gyrotrons. The underlying PDI process responsible for the observations involved only one trapped daughter wave, and the developed model predicted a power depletion of a few percent [25, 26].

5. Consequences of PDIs

So far, this paper has considered numerical simulations and experimental detections of PDIs. In this section, limitations on reactor systems, such as heating, current drive, and diagnostics, are discussed. The main concern of PDIs is the drain of injected wave power that is otherwise intended to be absorbed by the electrons near the cyclotron resonance but is instead transferred to waves with other propagation and absorption characteristics than those of the pump wave.

Historically, the occurrence of PDIs during microwave heating has mainly been considered in EBW heating and current drive experiments, where the convective instabilities discussed in sections 3.1 and 4.1 can occur. Signatures of this instability have been suggested to be a characteristic of the excitation of EBWs [27], and the relatively slow group velocity of EBWs compared to X-mode waves means that the power threshold for nonlinear wave effects is typically much smaller for EBWs. Nevertheless, no significant power loss has been reported in any experiment. EBWs remain of great interest for current drive in future spherical tokamaks such as the STEP device [28]. However, PIC simulations of EBWs in MAST-U suggest that PDIs and other nonlinear effects could be detrimental to the linear excitation of EBWs [29] in some cases. This may not be the case for STEP because the coupling to the EBWs is planned to occur between the fundamental and second-harmonic electron cyclotron frequency. In MAST-U, on the other hand, coupling to the EBW will occur between the second and third-harmonic electron cyclotron frequency, which allows other interactions to come into play [30].

It is important to note that even if PDIs can deplete the pump wave in severe cases, this does not necessarily mean that power would be lost from the plasma, as that would require the produced daughter waves to not interact with it. Rather, it may simply lead to absorption in other regions of the plasma, so an understanding of PDIs may be crucial in order to predict EBW power deposition profiles in devices like MAST-U. When EBW heating was demonstrated for the first time in an overdense H-mode plasma in a tokamak, there was a discrepancy between the predicted and measured power deposition profile [31]. Additionally, there have been a number of reports of anomalous microwave deposition profiles [32] and suprathermal electron populations in the outer parts of confined plasmas where no resonance was nearby [33]. It has been speculated that such observations could be caused by PDIs, although a direct link has not been established.

Convective PDIs also significantly limits the operation of collective Thomson scattering (CTS) on ASDEX Upgrade, which relies on detecting scattered radiation from a gyrotron to extract information about ion dynamics in the plasma. In this case, the injected O-mode reflects off the inner wall—similar to the mechanism described in section 4.1—and daughter waves within the CTS spectral range can be generated at the UH resonance. The daughter waves reaching the CTS radiometer are often orders of magnitude stronger than the scattered CTS signal, preventing straightforward identification of the CTS spectrum itself. This type of PDI can be mitigated by controlling the magnetic field and optimizing the plasma and gyrotron geometry to enhance absorption of the reflected X-mode, thereby reducing the power reaching the UH resonance to below the PDI threshold [34].

Although rarely considered, the occurrence of absolute TPD, generating trapped half-frequency waves during second-harmonic X-mode heating, can also cause problems. One issue is that a fraction of the gyrotron beam power is channeled to the half-frequency waves, potentially leading to unwanted power deposition in the plasma edge. The fraction of anomalous power absorption during TPD varies with the gyrotron power and plasma parameters. Experimental results from the Granite linear device have shown a power drain of a microwave beam due to TPD in a low-temperature plasma of 40% in steady state with transients up to 70% [35, 36], aligning with model predictions. Yet, up to now no significant power losses due to TPD have been reported from tokamaks or stellarators.

What has instead been reported numerous times are observations of unexpected suprathermal ion populations [37–40] and ion cyclotron emissions [41] in purely second-harmonic X-mode ECRH plasmas. In a recent study [42], measurements of suprathermal ions were correlated with the occurrence of TPD and the subsequent decay chain illustrated in figure 6. The generated ion Bernstein waves in the lower hybrid range are known to interact strongly with the ion population [43] and could be responsible for the observed ion acceleration. Thus, these measurements indicate that some energy is channeled from the electron cyclotron range of frequencies to the lower hybrid range of frequencies during TPD.

The presence of the absolute TPD instability may also inhibit the operation of various microwave diagnostics. The first documented case of interference between TPD and plasma diagnostics was reported in the electron cyclotron emission (ECE) system on the TEXTOR tokamak, where TPD prevented the determination of the electron temperature from ECE measurements and hindered the observation of electron dynamics associated with rotating magnetic islands [44]. Additionally, significant damage of microwave components correlated with TPD has been reported from ASDEX Upgrade [45]. This indicates that the power losses of the pump beam could be large, but perhaps more urgently that microwave sensitive equipment needs to be protected from escaping signatures of this instability.

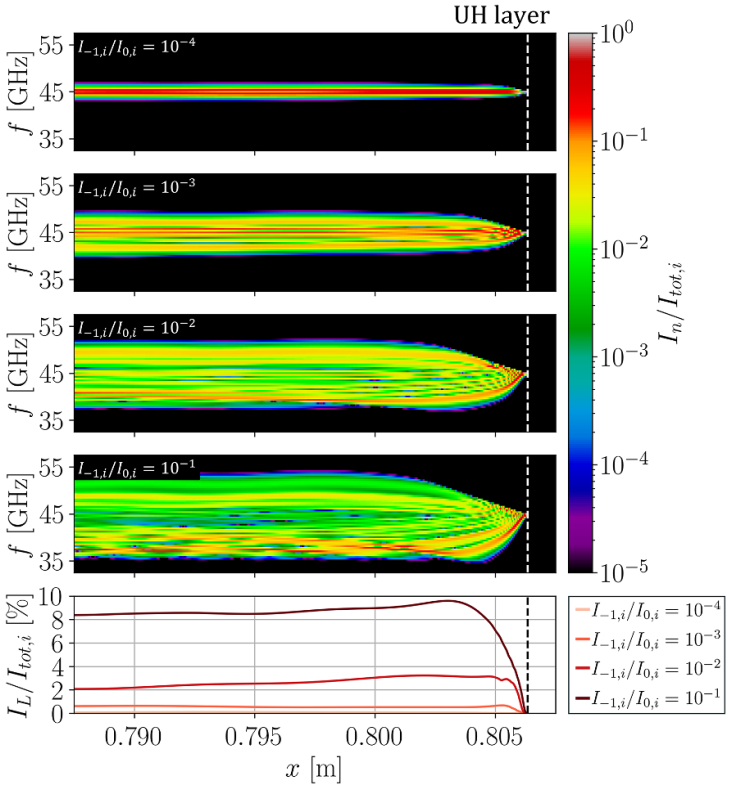

Figure 15. Intensities of a range of EBWs and the LH wave due to a cascaded parametric amplification process with four different seed wave intensities I_{-1} relative to that of the pump wave I_0. All waves are propagating from right to the left. The pump wave has an intensity of $I_0 = 50\,\mathrm{kW\,cm^{-2}}$ and a frequency of $f_0 = 45\,\mathrm{GHz}$, and the seed wave has a frequency of $f_{-1} = 44.62\,\mathrm{GHz}$. Reproduced from [10]. © The Author(s). Published by IOP Publishing Ltd. CC BY 4.0.

6. Potential exploitations of PDIs

The goal of most research on PDIs is to assess and possibly mitigate the associated consequences in a variety of heating schemes. As knowledge about PDIs improves through experiments, theoretical work, and numerical simulations, new ways to exploit PDIs have recently been suggested.

As was demonstrated in the previous sections, absolute PDIs can be caused by trapping of waves in nonmonotonic density structures. The occurrence of such PDIs as well as frequency shifts of the daughter waves are very sensitive to the properties of the density structure. One idea is therefore to use measurements of radiation from PDI daughter waves to diagnose density fluctuations around the second-harmonic UH resonance. An early effort to diagnose density fluctuations due to blob filaments in the plasma edge was presented in [46]. A similar procedure could be used to assess density perturbations in the plasma core, e.g. due to rotating magnetic islands, by moving the second-harmonic UH layer further into the plasma. This could be done by modifying the plasma density, the magnetic field, or simply by modifying the gyrotron frequency significantly. For such a method to be reliable, further advances in theoretical work are required.

Another intriguing feature of PDIs is that they present a way for energy flow between waves in the electron cyclotron range of frequencies, the lower hybrid range of frequencies, and the ion cyclotron range of frequencies. If PDI processes can be controlled, they could enable a channeling of energy from microwaves (e.g. from gyrotrons) to low-frequency waves. As is customary in many optical processes, it is possible to seed a convective parametric instability of the type shown in figure 5. A new study predicts that doing so can initiate a long cascade of PDIs, which can channel up to 12% of the total energy to high-harmonic ion Bernstein waves [10]. An example of this mechanism, called cascaded parametric amplification (CPA), is shown in figure 15. Here, the effects of four different seed wave amplitudes are considered in a simulated plasma that emulates the pedestal region of the ST-40 tokamak. At low seed wave intensities (top panel in figure 15), the energy is simply distributed among a few up- and down-shifted EBWs due to Stokes and anti-Stokes processes, as was seen in figure 5. Increasing the seed wave

amplitude initiates a long cascade of PDIs dominated by Stokes decays, resulting in a large amplification of the ion Bernstein waves. Pursuing the CPA method and similar controlled PDI schemes could potentially pave the way for ion heating using microwaves in the 100 GHz range.

7. Conclusions

In this work, we have introduced the concept of PDIs of microwave in the electron cyclotron resonance range of frequencies, with a focus on fusion plasmas. Using both PIC simulations and various experimental data, we have demonstrated that both convective and absolute instabilities can occur during ECRH in stellarators and tokamaks.

Convective instabilities are likely to arise when an X-mode wave reaches the UH resonance from the high-field side. While this scenario may happen in the uncommonly used high-field-side launched fundamental ECRH in X-mode, it can also occur under more typical circumstances. This includes fundamental or second-harmonic EBW O-X-B conversion planned for MAST-U, as well as in O-mode-based CTS experiments on ASDEX Upgrade.

Absolute instabilities may occur during second-harmonic X-mode ECRH, where daughter waves can become trapped in non-monotonic density perturbations near the second-harmonic UH resonance. Model cases predict power losses exceeding 50%, which have been confirmed in low-temperature plasmas. However, no significant reduction in heating or current drive efficiency has been observed to date in high-temperature tokamaks. Nevertheless, ion acceleration associated with PDIs has been observed at TCV, and unexplained ion acceleration in TJ-II has also been suggested to originate from PDIs. Although fundamental O-mode ECRH planned for ITER has been predicted to undergo PDI, this has not yet been experimentally verified and is therefore not addressed further in this work.

Finally, PDIs have also been proposed as a diagnostic tool for edge density fluctuations and is currently being investigated as a novel method for exciting high harmonics of ion Bernstein waves within plasmas.

Acknowledgments

This work was partially funded through the public-private partnership between Tokamak Energy and the Technical University of Denmark. This work has been supported by research Grant No. 15483 from VILLUM FONDEN, research Grant No. CF23-0181 from the Carlsberg Foundation, and research Grant Nos. NNF22OC0076017 and NNF24OC0087547 from the Novo Nordisk Fonden. This work has been carried out within the framework of the EUROfusion Consortium, partially funded by the European Union via the Euratom Research and Training Programme (Grant Agreement No 101052200 — EUROfusion). Views and opinions expressed are however those of the authors only and do not necessarily reflect those of the European Union or the European Commission. Neither the European Union nor the European Commission can be held responsible for them.

Data availability statement

The data that support the findings of this study are openly available at the following URL/DOI: https://doi.org/10.11583/DTU.27003109 [47].

Author contributions

S K Nielsen 0000-0003-4175-3829
Conceptualization (lead), Funding acquisition (lead), Supervision (lead)

References

[1] Erckmann V and Gasparino U 1994 Electron cyclotron resonance heating and current drive in toroidal fusion plasmas *Plasma Phys. Control. Fusion* **36** 1869–962
[2] Westerhof E *et al* 2009 Strong scattering of high power millimeter waves in tokamak plasmas with tearing modes *Phys. Rev. Lett.* **103** 125001

[3] Gusakov E Z and Popov A Y 2016 Theory of anomalous backscattering in second harmonic x-mode ECRH experiments *Phys. Plasmas* **23** 082503
[4] Gusakov E Z and Popov A Y 2019 Possibility of strong anomalous absorption of microwaves in electron cyclotron resonance heating experiments in fusion devices *Nucl. Fusion* **59** 104003
[5] Gusakov E Z and Popov A Y 2020 Low-power-threshold parametric decay instabilities of powerful microwave beams in toroidal fusion devices *Phys.-Usp.* **63** 365
[6] Senstius M G, Nielsen S K, Vann R G and Hansen S K 2019 Particle-in-cell simulations of parametric decay instabilities at the upper hybrid layer of fusion plasmas to determine their primary threshold *Plasma Phys. Control. Fusion* **62** 25010
[7] Senstius M G, Gusakov E Z, Yu Popov A and Nielsen S K 2022 Absolute parametric decay instabilities of X2 microwave beams in reduced models and fully kinetic codes *Plasma Phys. Control. Fusion* **64** 115001
[8] Popov A Y and Gusakov E Z 2015 Low-threshold absolute two-plasmon decay instability in the second harmonic electron cyclotron resonance heating experiments in toroidal devices *Plasma Phys. Control. Fusion* **57** 025022
[9] Hansen S K 2019 Parametric decay instabilities in the electron cyclotron resonance heating beams at ASDEX upgrade *PhD Dissertation* Technical University of Denmark (https://backend.orbit.dtu.dk/ws/portalfiles/portal/198805735/PhDThesisMaster.pdf)
[10] Clod A, Senstius M G, de Wit J K, Lopez N, Shevchenko V F and Nielsen S K 2026 Cascaded parametric amplification of lower hybrid waves using electron Bernstein waves *Nucl. Fusion* **66** 046033
[11] Senstius M G, Nielsen S K and Vann R G L 2021 Trapped upper hybrid waves as eigenmodes of non-monotonic background density profiles *Plasma Phys. Control. Fusion* **63** 065018
[12] Senstius M G, Nielsen S K and Vann R G L 2020 Numerical investigations of parametric decay into trapped waves in magnetized plasmas with a non-monotonic density background *Phys. Plasmas* **27** 062102
[13] de Wit J K, Senstius M G, Clod A, Ragona R and Nielsen S K 2025 Parametric decays into trapped microwaves in low-temperature laboratory plasmas *Plasma Phys. Control. Fusion* **67** 055026
[14] Arber T D *et al* 2015 Contemporary particle-in-cell approach to laser-plasma modelling *Plasma Phys. Control. Fusion* **57** 113001
[15] McDermott F S, Bekefi G, Hackett K E, Levine J S and Porkolab M 1982 Observation of the parametric decay instability during electron cyclotron resonance heating on the Versator II tokamak *Phys. Fluids* **25** 1488–90
[16] Shevchenko V, Cunningham G, Gurchenko A, Gusakov E, Lloyd B, O'Brien M, Saveliev A, Surkov A, Volpe F and Walsh M 2007 Development of electron Bernstein wave research in MAST *Fusion Sci. Technol.* **52** 202–15
[17] Laqua H P, Erckmann V, Hartfuß H J and Laqua H 1997 Resonant and nonresonant electron cyclotron heating at densities above the plasma cutoff by O-X-B mode conversion at the W7-AS stellarator *Phys. Rev. Lett.* **78** 3467–70
[18] Köhn A *et al* 2012 Schemes of microwave heating of overdense plasmas in the stellarator TJ-K *Plasma Phys. Control. Fusion* **55** 14010
[19] Hansen S K, Nielsen S K, Stober J, Rasmussen J, Salewski M and Stejner M (ASDEX Upgrade Team) 2019 Power threshold and saturation of parametric decay instabilities near the upper hybrid resonance in plasmas *Phys. Plasmas* **26** 062102
[20] Nielsen S K, Salewski M, Westerhof E, Bongers W, Korsholm S B, Leipold F, Oosterbeek J W, Moseev D and Stejner M 2013 Experimental characterization of anomalous strong scattering of mm-waves in TEXTOR plasmas with rotating islands *Plasma Phys. Control. Fusion* **55** 11
[21] Hansen S K, Nielsen S K, Stober J, Rasmussen J, Stejner M, Hoelzl M and Jensen T (ASDEX Upgrade Team) 2020 Parametric decay instabilities near the second-harmonic upper hybrid resonance in fusion plasmas *Nucl. Fusion* **60** 106008
[22] Senstius M G, Ragona R, Jacobsen A S, Rasmussen J, Hansen S K, Stober J, Salewski M, Akers R and Nielsen S K 2025 Parametric decay of a gyrotron beam due to a rotating magnetic island in Asdex Upgrade *Nucl. Fusion* **65** 026004
[23] Nielsen S K *et al* 2015 Measurements of the fast-ion distribution function at ASDEX upgrade by collective Thomson scattering (CTS) using active and passive views *Plasma Phys. Control. Fusion* **57** 035009
[24] Ragona R, Jacobsen A S, Jensen T, Jessen M, Pedersen A C, Gryaznevich M and Nielsen S K 2023 The second harmonic heating system for the NORTH tokamak *Fusion Eng. Des.* **194** 113839
[25] Tancetti A *et al* 2022 Nonlinear decay of high-power microwaves into trapped modes in inhomogeneous plasma *Nucl. Fusion* **62** 074003
[26] Tancetti A *et al* 2023 Inhibition of parametric decay in heating microwave beams during fluctuations of the density profile in the edge island of Wendelstein 7-x *Plasma Phys. Control. Fusion* **65** 015001
[27] Laqua H P 2007 Electron Bernstein wave heating and diagnostic *Plasma Phys. Control. Fusion* **49** R1–R42
[28] Wilson T, Freethy S, Henderson M, Köhn-Seeman A, Konoplev I, Saarelma S, Speirs D and Vann R (the STEP team) 2023 Electron Bernstein wave (EBW) current drive profiles and efficiency for step *EPJ Web Conf.* **277** 01011
[29] Senstius M G, Freethy S J and Nielsen S K 2023 Nonlinear degradation of O-X-B mode conversion in Mast Upgrade *EPJ Web Conf.* **277** 01009
[30] Senstius M G, Freethy S, Nielsen S K and Barnes M 2024 Nonlinear Landau damping of electron Bernstein waves in MAST-U *EPJ Web Conf.* **313** 01003
[31] Mueck A, Curchod L, Camenen Y, Coda S, Goodman T P, Laqua H P, Pochelon A, Porte L and Volpe F 2007 Demonstration of electron-Bernstein-wave heating in a tokamak via O-X-B double-mode conversion *Phys. Rev. Lett.* **98** 175004
[32] Andreev V F, Dnestrovskij Y N, Ossipenko M V, Razumova K A and Sushkov A V 2004 The ballistic jump of the total heat flux after ECRH switching on in the T-10 tokamak *Plasma Phys. Control. Fusion* **46** 319–35
[33] Killer C *et al* 2022 Observation of non-thermal electrons outside the SOL in the Wendelstein 7-X stellarator *Nuclear Materials and Energy* **33** 101274
[34] Nielsen A H *et al* 2017 Numerical simulations of blobs with ion dynamics *Plasma Phys. Control. Fusion* **59** 025012
[35] Altukhov A B, Arkhipenko V I, Gurchenko A D, Gusakov E Z, Popov A Y, Simonchik L V and Usachonak M S 2019 Observation of the strong anomalous absorption of the X-mode pump in a plasma filament due to the two-plasmon decay *Europhys. Lett.* **126** 15002
[36] Gusakov E Z, Popov A Y, Simonchik L V and Usachonak M S 2025 Strong anomalous absorption of an X-mode pump microwave in a plasma filament due to the two-plasmon decay instability *Phys. Plasmas* **32** 092101
[37] Pietrzyk Z A, Pochelon A, Behn R , Bondeson A, Dutch M, Goodman T P, Tran M Q and Whaley D R 1993 Electron cyclotron resonance heating on the TCA tokamak *Nucl. Fusion* **33** 197
[38] Rapisarda D, Zurro B, Tribaldos V and Baciero A (TJ–II team) 2007 The role of a fast ion component on the heating of the plasma bulk *Plasma Phys. Control. Fusion* **49** 309–24

[39] Coda S (for the TCV Team) 2015 The science program of the TCV tokamak: exploring fusion reactor and power plant concepts *Nucl. Fusion* **55** 104004
[40] Martínez M, Zurro B, Baciero A, Jiménez-Rey D and Tribaldos V 2018 Investigation of the role of electron cyclotron resonance heating and magnetic configuration on the suprathermal ion population in the stellarator TJ-II using a luminescent probe *Plasma Phys. Control. Fusion* **60** 025024
[41] Sumida S, Shinohara K, Ichimura M, Bando T, Bierwage A, Kobayashi T, Yamazaki H, Moriyama S and Ide S 2023 Observation of ion-cyclotron-range-of-frequency wave emission in electron-cyclotron-resonance-heated tokamak plasma *Plasma Phys. Control. Fusion* **65** 075002
[42] Clod A, Senstius M G, Nielsen A H, Ragona R, Thrysøoe A S, Kumar U, Coda S and Nielsen S K 2024 Cascades of parametric instabilities in the tokamak plasma edge during electron cyclotron resonance heating *Phys. Rev. Lett.* **132** 135101
[43] Castaldo C and Napoli F 2024 Nonlinear lower hybrid wave equations in collisional tokamak plasmas *Plasma Phys. Control. Fusion* **66** 95005
[44] Oosterbeek J W *et al* 2008 A line-of-sight electron cyclotron emission receiver for electron cyclotron resonance heating feedback control of tearing modes *Rev. Sci. Instrum.* **79** 093503
[45] Hansen S K *et al* 2021 Microwave diagnostics damage by parametric decay instabilities during electron cyclotron resonance heating in ASDEX upgrade *Plasma Phys. Control. Fusion* **63** 095002
[46] Clod A, Ragona R, Senstius M G, Jensen T, Kumar U, Coda S and Nielsen S K (the TCV Team) 2024 Utilizing parametric instabilities to diagnose edge density fluctuations in TCV *Plasma Phys. Control. Fusion* **66** 125001
[47] Nielsen S K, de Witt J K, Clod A, Rasmussen J, Senstius M and Ragona R 2026 Parametric decay instabilities of microwave beams in fusion plasmas: occurrence, consequences and new possibilities *data.dtu.dk* (https://doi.org/10.11583/DTU.27003109)